Available online at www.sciencedirect.com
SCIENCE DIRECT
International Journal of Heat and Mass Transfer 49 (2006) 1999–2008
International Journal of HEAT and MASS TRANSFER
www.elsevier.com/locate/ijhmt

Technical Note

The effect of the top and bottom wall temperatures on the laminar natural convection in an air-filled square cavity

W. Wu, D. Ewing, C.Y. Ching *

Department of Mechanical Engineering, McMaster University, Hamilton, Ont., Canada L8S 4L7

Received 14 July 2005; received in revised form 18 November 2005
Available online 28 February 2006

Abstract

The effect of the top and bottom wall temperatures on the natural convection heat transfer characteristics in an air-filled square cavity driven by a difference in the vertical wall temperatures was investigated by measuring the temperature distributions along the heated vertical wall and visualizing the flow patterns in the cavity. The experiments were performed at a horizontal Grashof number of 1.9×10^8. Increasing the top wall temperature resulted in a separated flow region on the top wall, which caused a secondary flow between the separated flow and the boundary layer on the heated vertical wall. This secondary flow had a significant effect on the heat transfer in this region. Changes in the top and bottom wall temperatures changed the temperature gradient and the average temperature of the air outside the thermal boundary layers in the cavity. The local heat transfer along much of the heated vertical wall could be correlated by $Nu = C \cdot Ra^{0.32}$, but the constant C increased when the average of the top and bottom wall temperatures increased.

Keywords: Natural convection; Square cavity; Stable stratification

1. Introduction

There have been numerous investigations of the natural convection heat transfer that occurs in an enclosure due to a temperature difference across the enclosure. Most of the early investigations of this problem, reviewed in Ostrach [1] or Yang [2], focused on the heat transfer in rectangular or cylindrical enclosures [3–7]. More recent investigations have focused on characterizing the natural convection in enclosures with more complex boundary conditions or geometries, including convection in rectangular enclosures inclined relative to the gravity force [8–10], enclosures with non-uniform or three-dimensional temperature distributions on the walls [11–13], or enclosures with partitions or fins [14–16]. In all cases, there was heat transfer in the cavity due to natural convection flows in boundary layers along the walls for sufficiently large horizontal Grashof numbers.

The air in the core region of cavities with nominally adiabatic top and bottom walls are stably stratified, with the temperature increasing with height. This affects the buoyancy force in the natural convection boundary layers that develop along the vertical wall. The temperatures of the top and bottom walls also affect the stratification rate and natural convection in the cavity. For example, Ostrach and Raghavan [17] visualized the flow patterns in square and rectangular enclosures containing silicone oil with a hot upper wall and cooled lower wall in addition to a temperature difference across the vertical walls. The resulting flow pattern in the cavity became more asymmetric as the temperature difference between the horizontal walls increased relative to that between the vertical walls, eventually causing a secondary recirculating flow region to occur near the top of the vertical wall for large temperature differences. Shiralkar and Tien [18] performed a similar numerical investigation of the heat transfer in an air-filled square enclosure for cases where the top and bottom walls

* Corresponding author. Tel.: +1 905 5259140; fax: +1 905 572 7944.
E-mail address: chingcy@mcmaster.ca (C.Y. Ching).

0017-9310/$ - see front matter © 2006 Elsevier Ltd. All rights reserved.
doi:10.1016/j.ijheatmasstransfer.2005.11.027

Nomenclature

C	constant in the Nusselt Rayleigh number correlation, $Nu = C \cdot Ra^n$
g	gravity constant, m/s^2
Gr_L	horizontal Grashof number, $Gr_L = \frac{g\beta(T_H - T_C)L^3}{\nu^2}$
Gr_V	vertical Grashof number, $Gr_V = \frac{g\beta(T_T - T_B)H^3}{\nu^2}$
h	local heat transfer coefficient, W/m^2 °C
$\bar{h}$	average heat transfer coefficient for the vertical wall, W/m^2 °C
H	height of the cavity, m
k	thermal conductivity of the air, W/m °C
L	length of the cavity in the horizontal direction, m
n	exponent in the Nusselt Rayleigh number correlation, $Nu = C \cdot Ra^n$
Nu	local Nusselt number, $Nu = \frac{hy}{k}$
$\overline{Nu}_H$	average Nusselt number for the vertical wall, $\overline{Nu}_H = \frac{\bar{h}H}{k}$
q''	local heat flux, W/m^2
Ra	local Rayleigh number, $Ra = \frac{g\beta(T_H - T_\infty)y^3}{\alpha\nu}$
T_B	average temperature of the bottom wall in the cavity, °C
T_C	average temperature of the cooled vertical wall in the cavity, °C
T_H	average temperature of the heated vertical wall in the cavity, °C
T_T	average temperature of the top wall in the cavity, °C
T_∞	local ambient temperature outside of the boundary layer, °C
x	distance from the heated vertical wall, m
y	height above the bottom wall, m
α	thermal diffusivity, m^2/s
β	volume expansion coefficient at constant pressure, K^{-1}
$\theta_T - \theta_B$	difference between the non-dimensional top and bottom wall temperature
θ_∞	non-dimensional local ambient temperature outside the boundary layer, $\theta_\infty = \frac{(T_\infty - T_C)}{(T_H - T_C)}$
$d\theta_\infty/d(y/H)$	vertical gradient of the non-dimensional temperature outside the boundary layer on the heated vertical wall
ν	kinematic viscosity, m^2/s

Subscripts

B	bottom wall of the cavity
C	cooled vertical wall of the cavity
H	heated vertical wall of the cavity
T	top wall of the cavity

were heated or cooled. In this case, the temperature difference in the vertical direction was 2–5 times that in the horizontal direction. There was again a significant secondary flow near the top corner of the heated vertical wall. Somewhat surprisingly, the heat transfer from the heated vertical wall increased when the top wall was heated and the bottom wall was cooled even though the vertical velocity of the flow along the vertical walls decreased. Ravi et al. [19] later carried out a numerical investigation to examine how the change in the temperature of the horizontal wall altered the flow in a square cavity for cases with more modest temperature difference. They found that relatively modest changes in temperature of the top and bottom walls of the cavity (relative to that between the vertical walls) resulted in significant changes in the flow pattern in the cavity, particularly at the upper corner where the heated walls met and the lower corner where the cooled walls met. In particular, a recirculating flow pattern developed in these corners that became more pronounced as the temperature of the top wall increased, or the bottom wall decreased.

Heretofore, however, there does not appear to have been any experimental investigation that examined how the natural convection flow in an air-filled cavity driven by a temperature difference in the vertical walls changes as the temperature of the top and bottom wall of the cavity change. The objective of this investigation was to experimentally characterize how the flow and temperature distribution in a square cavity are affected by the change in the temperature of the horizontal walls in the cavity. The measurements were performed for a square enclosure for cases when the top wall of the cavity was heated and the bottom wall cooled. The experimental facility and experimental procedure used in this investigation are outlined in the next section. The results of the experiments are given in Section 3 and then the conclusions are presented.

2. Experimental methodology

The experiments in this investigation were performed using the cavity shown in Fig. 1. The cavity had a height of 305 mm and a width that could be varied from 100 to 610 mm by moving the right wall of the cavity. The width of the cavity was set to 305 mm, equal to the cavity height, for the measurements reported here. The cavity had a depth of 914 mm or 3 times the height so the flow should be approximately two-dimensional following Ostrach and Raghavan [17]. The walls of the cavity were designed so that one vertical wall and the top wall could be heated, while the other vertical wall and the bottom wall could be cooled. The end walls of the cavity contained two glass windows that allowed the flow in the enclosure to be visualized.

The heated top and left vertical walls were constructed using 12.7 mm aluminium plates, that were divided into

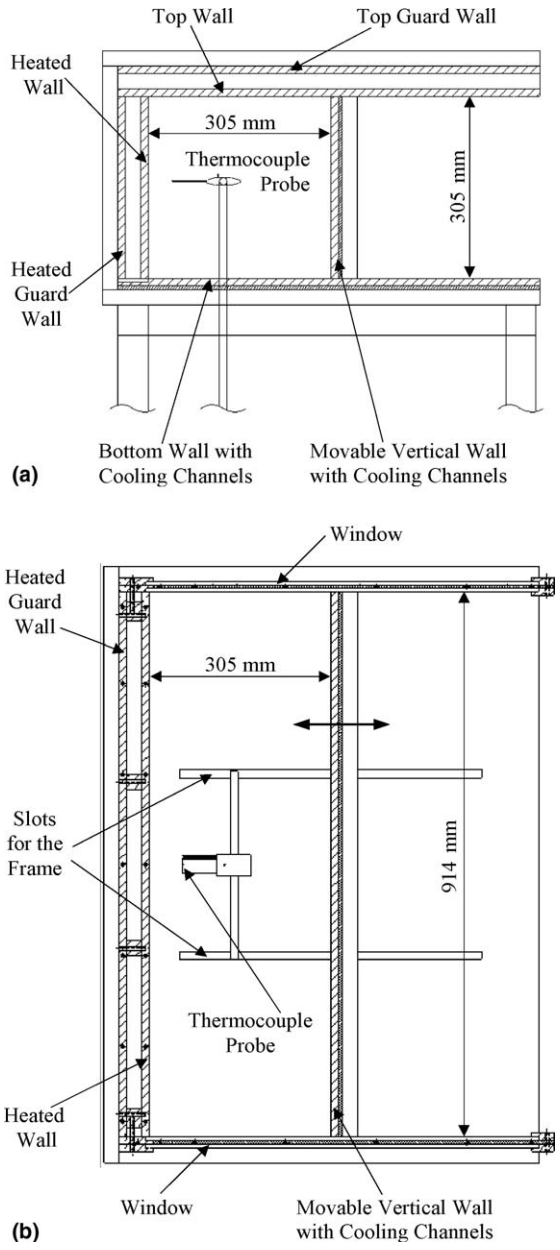

Fig. 1. Schematic of the enclosure from (a) the side view and (b) the top view.

sections by milling 6 mm grooves on the outside surface of these plates. The top wall was divided into four equal size sections, while the vertical wall was divided into three sections that were 89 mm, 102 mm, and 114 mm high, respectively, with the smallest section at the bottom of the wall where the heat flux into the cavity was the largest. Silicone rubber heaters, with a maximum capacity of 180 W, were embedded into 25 mm wide grooves machined in the center of each section, and powered using a multi-channel variable duty controller. These heated plates were insulated using aluminium guard heater walls that were split into sections, similar to the inner walls. The walls were separated by a 25 mm thick layer of insulation, with an additional layer outside of the guard walls.

The cooled bottom and right vertical walls were also constructed from 12.7 mm thick aluminium plates that contained two 25 mm × 6 mm serpentine cooling channels machined into the face. The channels were closed using 6.4 mm thick outer aluminium plates that contained the inlets and outlets for the channels, and were insulated from the outside using a 25 mm thick layer of insulation. The flow rate of cold water through each of the channels and the water inlet and outlet temperatures were measured using rotameters and T-type thermocouples, respectively. The junction between the heated vertical wall and the top wall of the cavity was insulated using a thin layer of mineral fiber paper. The heated vertical wall was isolated from the bottom wall of the cavity by supporting the vertical guard wall on four small Delrin blocks, so that an air gap approximately 1 mm high was left between the inner walls.

The temperature distributions in the heated and cooled walls were measured using 0.25 mm (0.010″) T-type thermocouples that are described in more detail in [20]. The temperatures along the centerline were monitored continuously through the experiment and these measurements were used to compute the average wall temperatures reported here. The temperature distribution of the air inside the cavity was measured using a 0.051 mm (0.002″) diameter T-type thermocouple probe mounted between two 1.5 mm diameter tubes that were 57 mm long and 29 mm apart so they would not interfere with the flow near the measurement location. The thermocouple probe unit was mounted on a traverse that could move in both the horizontal and vertical directions. The position of the thermocouple relative to the walls in the cavity was determined using two positioning rods that closed an electrical circuit when they touched the wall. The distance between the thermocouple bead and the tip of the horizontal positioning rod was measured using a microscope.

In each experiment, the power to the heaters and the cooling water flow rates were adjusted until the inner walls reached the desired temperatures. The power to the guard heaters was also adjusted so that the local temperature difference between the guard wall and the corresponding inner wall was less than 1.5 °C. Measurements were started after the wall temperatures varied less than ±0.5 °C for over 1 h, as in Chinnakotla et al. [21]. The temperature profiles near the heated vertical wall in the cavity were then measured at 9 heights 25 mm apart. The measurements of the instantaneous temperature were averaged for 20 s at each point.

The flow field in the upper corner of the cavity was visualized using smoke that was illuminated by a laser light sheet. Incense smoke, cooled to approximately room temperature, was injected slowly through one of the two slots machined in the bottom wall for the traverse. Care was taken to ensure the injection of the smoke was slow enough to allow it to follow the flow inside the cavity. A digital camera positioned outside the window of the sidewall of the cavity was used to record the resulting smoke pattern.

The local heat flux from the heated vertical wall was estimated from the slope of the temperature profile in the near-wall region of the boundary layer, where conduction was the dominant mode of heat transfer and the slope was approximately constant. In all cases, there were at least seven measurement points in this region. The thermal conductivity of the air, k, was evaluated at the average temperature in this near-wall region. The local heat flux was then used to determine the local heat transfer coefficient given by

$$h = \frac{q''}{(T_H - T_\infty)}. \quad (1)$$

The local temperature of the heated wall was determined by projecting the temperature profiles to the wall.

The uncertainties in the measurements reported here were evaluated using the approach outlined by Coleman and Steele [22]. It was found that the uncertainty in the local heat flux was 3–5%, the uncertainties in the local heat transfer coefficient and the local Nusselt number were 5–8%, and the uncertainty in the local Rayleigh number was 4–5%.

3. Results and discussion

The natural convection in the square enclosure was initially examined for the case where the top and bottom walls were insulated and the average temperatures of the vertical walls in the enclosure were held at 82 °C and 14 °C. The horizontal Grashof number based on the width of the cavity in this case was 1.9×10^8. The normalized temperature profiles measured at different positions along the heated vertical wall of the cavity are shown in Fig. 2(a). It is clear that there is a thin thermal boundary layer near the heated vertical wall that grows in thickness as the flow travels up the wall, as expected. The temperature profiles outside of the boundary layer region were approximately uniform indicating there was not a significant natural convection flow outside of this thermal boundary layer. However, the temperature outside the boundary layer increases with height so most of the air in the cavity was stably stratified reducing the local buoyancy force acting on the flow in the boundary layer as it travels up the heated vertical wall. The temperature profiles between $y/H = 0.5$ and $y/H = 0.8$ had an undershoot near the edge of the boundary layer, where the local temperature fell below the local temperature in the core region of the cavity. A similar undershoot was observed by Tian and Karayiannis [23] in their temperature profiles measured for the natural convection in a square cavity with $Gr_L = 2.22 \times 10^9$. Cheesewright [24] noted that this occurred in natural convection boundary layers in non-isothermal surroundings because the heat flux to the fluid in the outer region of the boundary layer was not sufficient to change its temperature as quickly as the temperature outside the boundary layer.

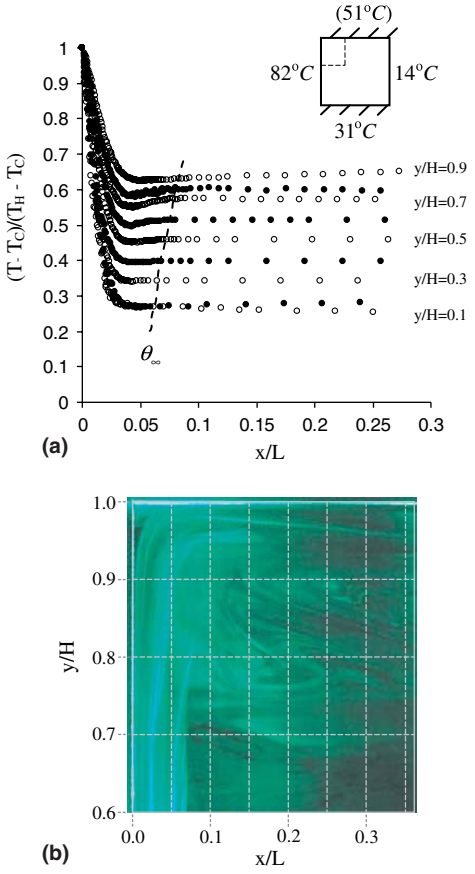

Fig. 2. (a) Non-dimensional temperature profiles in the cavity with insulated top and bottom wall for $Gr_L = 1.9 \times 10^8$ and (b) flow pattern in the upper corner where the heated vertical wall and the top wall meet.

The change in the non-dimensional temperature of the core region of the cavity observed here differed from that in the experiment with analogous boundary conditions by Tian and Karayiannis [23]. This difference may be due to differences in the way the bottom wall was insulated in

Table 1
Summary of the wall temperatures, Grashof numbers, and parameters in the correlation $Nu = C \cdot Ra^n$ for the cases studied in this investigation

Case	T_H (°C)	T_C (°C)	T_T (°C)	T_B (°C)	Gr_L	Gr_V	n	C
1	82	14	51 (insulated)	31 (insulated)	1.87×10^8	6.1×10^7	0.32	0.155
2	80	13	79	13	1.88×10^8	1.9×10^8	0.32	0.165
3	83	16	52 (insulated)	16	1.81×10^8	1.2×10^8	0.32	0.15
4	80	15	80	32 (insulated)	1.8×10^8	1.2×10^8	0.32	0.17
5	83	13	71	12	1.93×10^8	1.8×10^8	0.32	0.16
6	80	13	89	13	1.88×10^8	2.0×10^8	0.32	0.185
7	82	14	109	14	1.87×10^8	2.2×10^8	0.32	0.19

the two experiments. In particular, the non-dimensional temperature of the bottom wall $(T_B - T_C)/(T_H - T_C)$ was 0.25 for the current experiment, but was 0.39 for the results reported by Tian and Karayiannis [23]. The non-dimensional temperature on the top wall $(T_T - T_C)/(T_H - T_C)$ was, however, 0.54 in both experiments.

The visualization of the flow in the upper corner shown in Fig. 2(b) suggests there is some evidence of recirculating flow outside the boundary layers along the heated vertical wall and the top wall as reported by Olson et al. [25] and Tian and Karayiannis [23]. For the most part, however, the flow moves along the wall, and seems to travel around

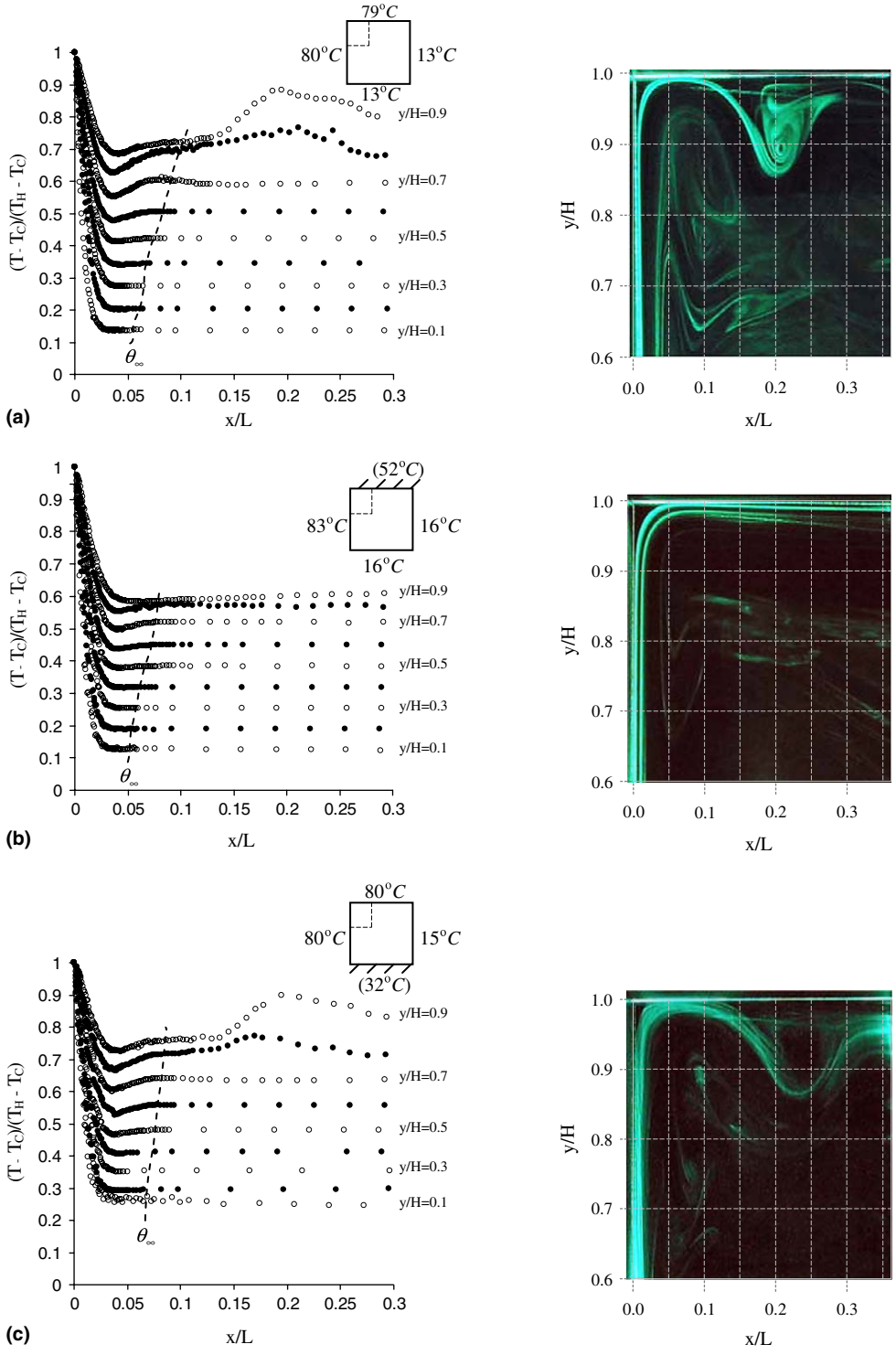

Fig. 3. Comparison of the temperature profiles in the cavity (Left), and flow patterns in the upper corner region (Right) for the cases where T_T and T_B were (a) 79 °C and 13 °C, (b) 52 °C (insulated) and 16 °C, and (c) 80 °C and 32 °C (insulated).

the corner without any evidence of separation. Ravi et al. [19] noted a similar circulation of fluid in the core region. However, they found there was a thickening of the boundary layer on the top wall after the flow travelled around the corner, and this difference may be due to differences in the temperature of the 'insulated' top wall.

The effect of changing the average temperatures of the top and bottom wall was initially examined for three cases. In the first case, the average temperatures of the top and bottom walls were approximately equal to the temperatures of the vertical walls, and in the second and third cases the bottom or top wall was insulated while the other wall was maintained at the temperature of the heated or cooled vertical wall. In all cases, the average temperatures of the vertical walls were maintained at approximately 82 °C and 14 °C, respectively, as summarized in cases 2–4 in Table 1. The temperature profiles along the heated vertical wall and the corresponding flow pattern in the upper corner of the cavity for these three cases are shown in Fig. 3. In all cases, there is a thin thermal boundary layer near the heated vertical wall, but the temperature distribution of the air outside the boundary layer changed as the temperatures of the top and bottom wall were changed. Further, in the cases where the top wall was heated (Fig. 3a and c), the temperature of the air outside the boundary layer near the top wall was not uniform and increased significantly. In these cases, the flow visualization shows a separated flow region on the top wall. This causes a secondary flow in the region between the separated flow on the top wall and the boundary layer on the heated vertical wall. There was a good correspondence between the variation of the temperature profiles and the flow visualization near the top of the cavity. Thus, it suggests that the non-uniformity in the temperature profiles at $x/L \geqslant 0.15$ near the top of the cavity is a measure of the separated boundary layer on the top wall. This occurred for both bottom wall temperatures suggesting that this was to a large extent a local phenomenon determined by the temperature of the top wall. The temperature of the air outside the boundary layer in the bottom section of the cavity decreased significantly when the temperature of the bottom wall was decreased, and thus did lower the temperature of the fluid in the core region somewhat, even up to $y/H = 0.7$.

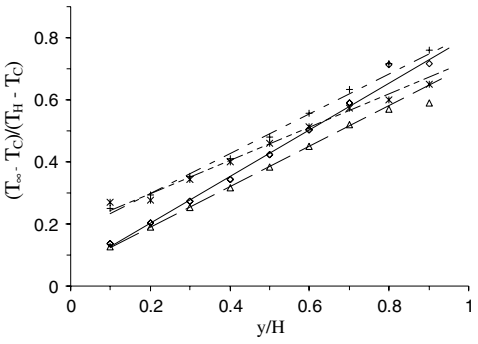

Fig. 4. Comparison of the non-dimensional temperature outside the boundary layer for the cases where T_T and T_B were ∗: 51 °C (insulated) and 31 °C (insulated), △: 52 °C (insulated) and 16 °C, +: 80 °C and 32 °C (insulated), and ◇: 79 °C and 13 °C.

The change in the non-dimensional temperature just outside the boundary layer with height for the above four cases is shown in Fig. 4. The temperatures just beyond the undershoot in the temperature profiles shown in Figs. 2 and 3 were used here as a measure of the local ambient temperature outside the boundary layer. This temperature was also used near the top wall since the flow visualization experiments showed that the higher temperature further from the heated vertical wall in these cases was actually a measure of the flow on the upper wall. In all four cases, the temperature outside the boundary layer increased approximately linearly with the height over most of the cavity. The exception was near the top wall when it was heated. In these cases, the temperature outside the boundary layer was approximately constant, likely due to mixing caused by the secondary flow in the region between the boundary layer on the heated vertical wall and the separated flow on the top wall. The temperature near the bottom wall was relatively independent of the top wall temperature.

The effect that the top wall temperature had on the natural convection flow in the cavity was investigated further by performing measurements for three additional cases with top wall temperatures of 71 °C, 89 °C, and 109 °C. The bottom wall was cooled in these cases in order to control this boundary condition, while the temperatures of the vertical walls were approximately 81 °C and 13 °C as summarized in cases 5–7 in Table 1. The non-dimensional temperature profiles measured along the heated vertical wall along with the corresponding flow patterns observed in the upper corner for these cases are shown in Fig. 5. The temperature profiles outside the boundary layer near the top of the cavity and the flow on the top wall changed as the temperature of the top wall in the cavity was increased. In particular, when the temperature of the top wall was 71 °C the temperature profiles at $y/H = 0.8$ and 0.9 were relatively uniform immediately outside the boundary layer on the heated vertical wall, but there were non-uniformities beyond $x/L = 0.15$. This corresponded to the separated flow region observed on the top wall in this case. The non-uniformity in the temperature profiles near the top of the cavity and the separated flow region on the top wall increased in size and moved toward the heated vertical wall as the temperature of the top wall was increased from 71 °C to 109 °C. The secondary flow formed between the separated flow on the top wall and the boundary layer on the heated vertical wall was reduced in width as the temperature of the top wall increased. This change affected the temperature distribution in the secondary flow just outside of the boundary layer at $y/H = 0.8$ and 0.9. In particular, the temperature in this region increased with height for the smaller top wall temperature, but was approximately constant for the larger temperatures, most likely because

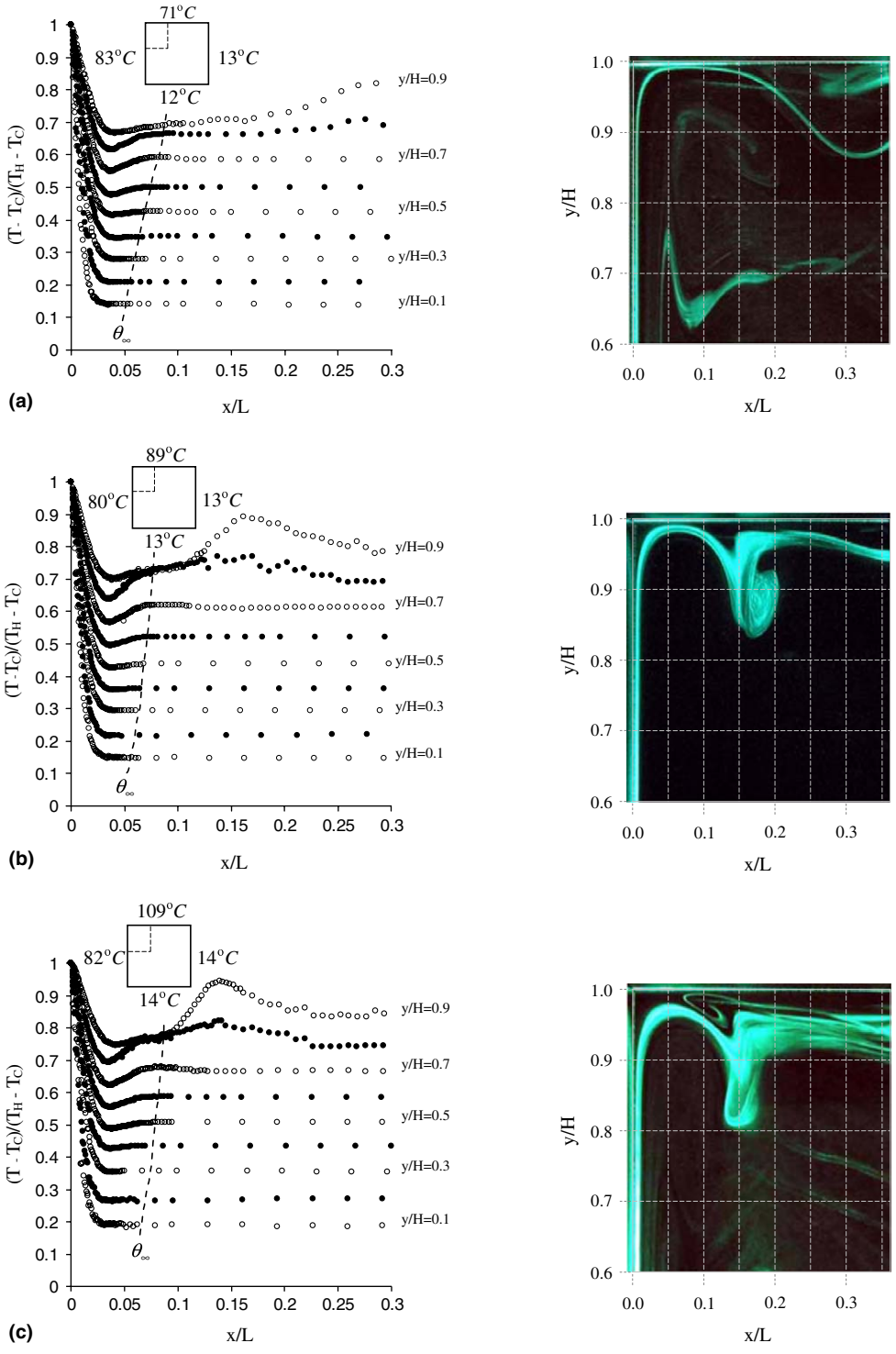

Fig. 5. Comparison of the temperature profiles in the cavity (Left), and flow patterns in the upper corner region (Right) for the cases where T_T and T_B were (a) 71 °C and 12 °C, (b) 89 °C and 13 °C, and (c) 109 °C and 14 °C.

the secondary flow is stronger when the separated flow is closer to the vertical wall.

The change in the non-dimensional temperature outside the boundary layer with height for the three cases in Fig. 5 and the two cases in Fig. 3a and b with the same bottom wall temperature is shown in Fig. 6. The results show again that the temperatures outside the boundary layer on the bottom part of the heated vertical wall increases approximately linearly with the height in all the cases. The temperature of the air near the bottom wall was essentially independent of the top wall temperature, so the stabilizing temperature gradient in the cavity increased with an increase of the top wall temperature. The change in the temperature gradient $d\theta_\infty/d(y/H)$ with the change in the

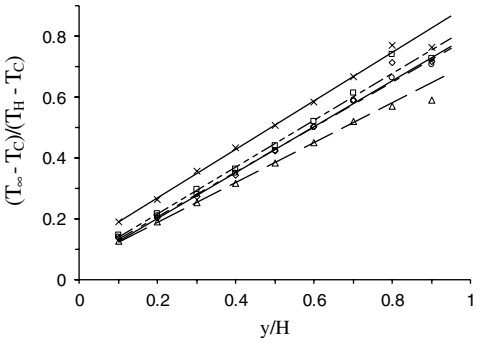

Fig. 6. Comparison of the non-dimensional temperature outside of the boundary layer for the cases where T_T and T_B were △: 52 °C (insulated) and 16 °C, ○: 71 °C and 12 °C, ◊: 79 °C and 13 °C, □: 89 °C and 13 °C, and ×: 109 °C and 14 °C.

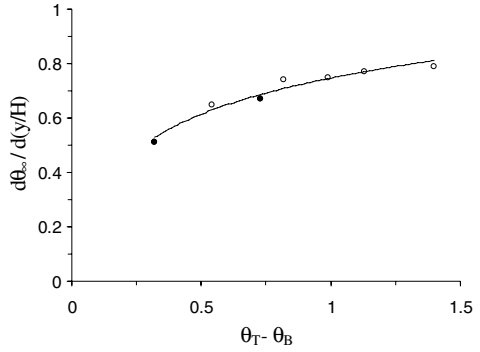

Fig. 7. Change in the vertical gradient of the temperature outside the boundary layer on the heated vertical wall with the temperature difference between the top and bottom walls for the cases with ○: a cooled bottom wall, and ●: an insulated bottom wall.

top wall temperature is shown in Fig. 7. The temperature gradient was determined by a linear fit to the data between $y/H = 0.1$ and 0.7 for the cases shown in Fig. 6. The results for the cases with the different bottom wall temperatures are also included in Fig. 7. It is clear that the vertical temperature gradient outside the boundary layer over much of the heated vertical wall increases as the difference between the top and bottom wall temperatures increases, but it does not appear to be directly proportional to this difference.

The local heat flux from the heated vertical wall, q'' (determined from the temperature profiles) for the five cases with different top wall temperature and cooled bottom wall is shown in Fig. 8(a). The local heat flux into the cavity from the heated vertical wall decreases as the flow develops along the wall as expected. The change in the top wall temperature had a significant effect on the heat transfer near the top of the heated vertical wall, where the local heat flux decreased by up to 40% when the temperature of the top wall was increased from 52 °C to 109 °C. The heat transfer near the bottom of the heated vertical wall also changed, but in these cases there was no obvious trend in the data. The effect of changing the bottom wall temperature on the heat flux is shown in Fig. 8(b). The

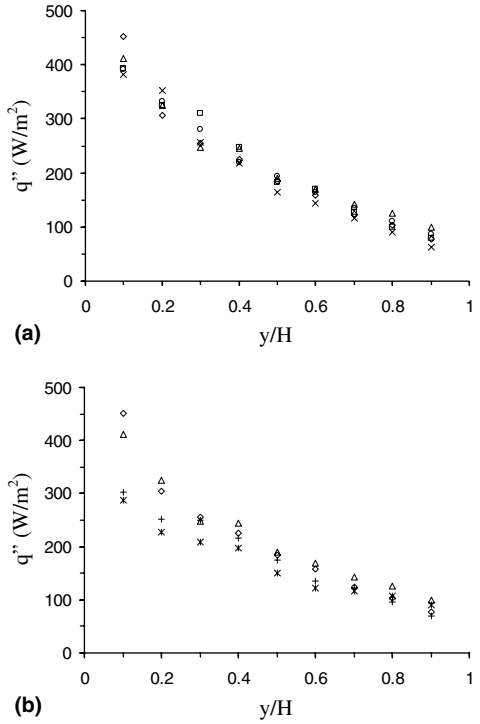

Fig. 8. Comparison of the local heat flux along the heated vertical wall (a) for the cases where T_T and T_B were △: 52 °C (insulated) and 16 °C, ○: 71 °C and 12 °C, ◊: 79 °C and 13 °C, □: 89 °C and 13 °C, and ×: 109 °C and 14 °C, and (b) for the cases where T_T and T_B were ∗: 51 °C (insulated) and 31 °C (insulated), △: 52 °C (insulated) and 16 °C, +: 80 °C and 32 °C (insulated), and ◊: 79 °C and 13 °C.

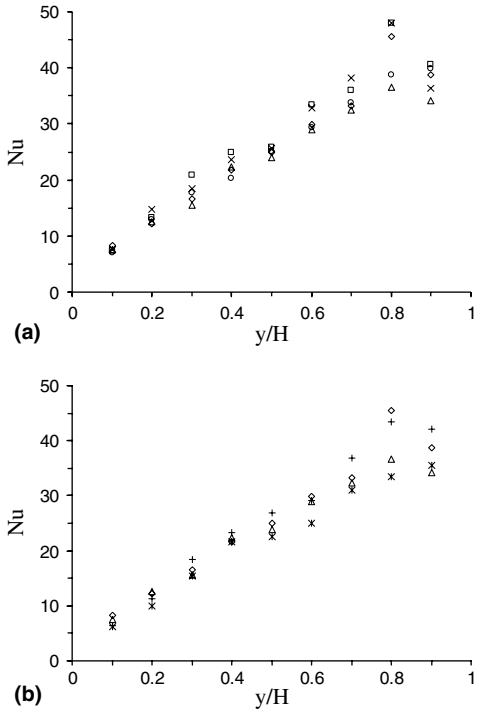

Fig. 9. Comparison of the local Nusselt number along the heated vertical wall (a) for the cases with different top wall temperatures and cooled bottom wall (symbols are the same as in Fig. 8), and (b) for the cases with different top and bottom wall temperatures (symbols are the same as in Fig. 8).

results show that the heat flux over the entire heated vertical wall increased when the temperature of the bottom wall on the cavity was reduced. The local heat flux was increased by up to 50% near the bottom of the heated vertical wall, but by only 10% near the top of the wall.

The change in the local Nusselt number profile along the heated vertical wall with the change in the top wall temperature is shown in Fig. 9(a). The local Nusselt number increased along the wall up to $y/H = 0.8$, before decreasing. The significant increase in the Nusselt number at $y/H = 0.8$ when the top wall temperature was increased is likely due to the change in the secondary flow in the corner region. For example, the large increase in the local Nusselt number observed when the temperature of the top wall was increased from 71 °C to 79 °C corresponds to the onset of the strong secondary flow in the corner region. It should be noted that the local Nusselt number at $y/H = 0.8$ and 0.9 was evaluated using the temperature in the secondary flow just outside the boundary layer. Had the temperature from the separated flow region on the top wall be chosen instead, T_∞ would have been larger and the value of the local Nusselt number higher. The effect of the change in the bottom wall temperature on the local Nusselt number is shown in Fig. 9(b). The Nusselt numbers near the bottom wall ($y/H = 0.1$ and 0.2) were increased by 20–30% when the temperature of the bottom wall was reduced, indicating the increase in the heat flux in this region may not be simply due to the reduction in the local air temperature.

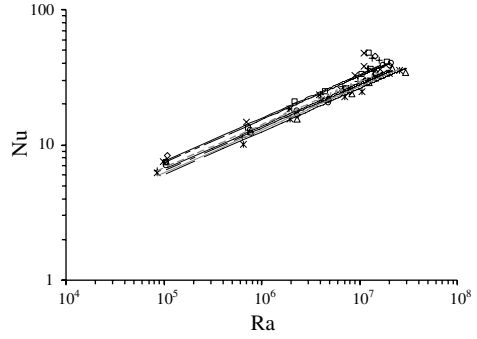

Fig. 10. Change in the local Nusselt number with the local Rayleigh number for all seven cases. Symbols are the same as in Fig. 8.

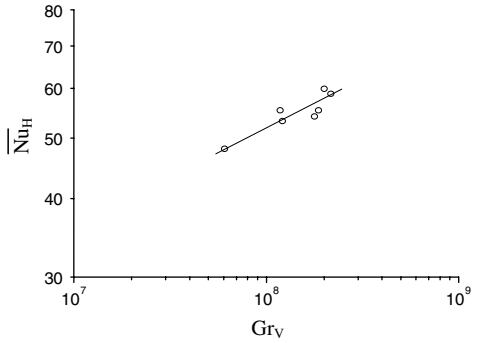

Fig. 11. Change in the average Nusselt number for the heated vertical wall with the vertical Grashof number.

The change in the local Nusselt number with the local Rayleigh number for all seven cases studied here is shown in Fig. 10. For $y/H \leqslant 0.7$, the results could be correlated by $Nu = C \cdot Ra^n$ with a value of $n = 0.32$. However, the value of the constant C in the correlation changed when the temperatures of the top and bottom wall were changed. The constant C increased from 0.15 to 0.19 as the temperature of the top wall on the cavity was increased from 52 °C to 109 °C, and decreased when the temperature of the bottom wall was decreased (see Table 1).

The change in the average Nusselt number for the heated vertical wall $\overline{Nu}_H$ with the vertical Grashof number Gr_V is shown in Fig. 11. The average Nusselt number increases with the vertical Grashof number, as found by Shiralkar and Tien [18]. The correlation between $\overline{Nu}_H$ and Gr_V was given by

$$\overline{Nu}_H = 3.58 \cdot Gr_V^{0.145} \tag{2}$$

with $Gr_L = 1.9 \times 10^8$ and Gr_V in the range 6.1×10^7–2.2×10^8 for the cases examined here.

4. Conclusions

An experimental investigation was performed to examine the effect of changes in the top and bottom wall temperatures on the natural convection in an air-filled square cavity driven by a temperature difference between the vertical walls. The experiments were performed at a horizontal Grashof number of 1.9×10^8, and top and bottom wall temperatures in the range 52–109 °C and 12–32 °C, respectively. The top wall temperature had a significant effect on the flow along the top wall. In particular, there was a flow separation on the top wall when the temperature of the top wall was increased. The location of this separated flow region moved toward the heated vertical wall as the temperature of the top wall was further increased, causing a significant secondary flow between the separated flow and the boundary layer on the heated vertical wall. This secondary flow had a significant effect on the heat transfer in the corner region, with the local Nusselt number increasing with the top wall temperature.

The change in the top and bottom wall temperatures also affected the temperature of the air outside of the thermal boundary layers in the cavity. The temperature gradient in the vertical direction outside the boundary layer on the heated vertical wall up to about $y/H = 0.7$ increased with an increase in the temperature difference between the top and bottom walls. The correlation between the local Nusselt number and the local Rayleigh number over this region of the heated vertical wall had the form $Nu = C \cdot Ra^{0.32}$, where the value of the constant C increased when the temperature difference between the top and bottom wall increased. The average Nusselt number for the heated vertical wall also increased when the vertical Grashof number Gr_V increased and could be

correlated by $\overline{Nu}_H = 3.58 \cdot Gr_V^{0.145}$ for the range of experiments performed here.

Acknowledgement

The support of the Natural Sciences and Engineering Research Council (NSERC) of Canada and Pratt & Whitney Canada is gratefully acknowledged.

References

[1] S. Ostrach, Natural convection in enclosures, J. Heat Transfer 110 (1988) 1175–1190.
[2] K.T. Yang, Transitions and bifurcations in laminar buoyant flows in confined enclosures, J. Heat Transfer 110 (1988) 1191–1204.
[3] E.R.G. Eckert, W.O. Carlson, Natural convection in an air layer enclosed between two vertical plates with different temperatures, Int. J. Heat Mass Transfer 2 (1961) 106–120.
[4] A. Emery, N.C. Chu, Heat transfer across vertical layers, J. Heat Transfer 87 (1965) 110–114.
[5] S. Weinbaum, Natural convection in horizontal cylinders, J. Fluid Mech. 18 (1964) 409–448.
[6] I.H. Brooks, S. Ostrach, An experimental investigation of natural convection in a horizontal cylinder, J. Fluid Mech. 44 (1970) 545–561.
[7] D.E. Cormack, L.G. Leal, J.H. Seinfeld, Natural convection in a shallow cavity with differentially heated end walls, Part 2. Numerical solutions, J. Fluid Mech. 65 (1974) 231–246.
[8] F.J. Hamady, J.R. Lloyd, H.Q. Yang, K.T. Yang, Study of local natural convection heat transfer in an inclined enclosure, Int. J. Heat Mass Transfer 32 (1989) 1697–1708.
[9] S.M. Elsherbiny, Free convection in inclined air layers heated from above, Int. J. Heat Mass Transfer 39 (1996) 3925–3930.
[10] M.A.R. Sharif, W. Liu, Numerical study of turbulent natural convection in a side-heated square cavity at various angles of inclination, Numer. Heat Transfer, Part A 43 (2003) 693–716.
[11] V. Erenburg, A.Y. Gelfgat, E. Kit, P.Z. Bar-Yoseph, A. Solan, Multiple states, stability and bifurcations of natural convection in a rectangular cavity with partially heated vertical walls, J. Fluid Mech. 492 (2003) 63–89.
[12] W.H. Leong, K.G.T. Hollands, A.P. Brunger, Experimental Nusselt numbers for a cubical-cavity benchmark problem in natural convection, Int. J. Heat Mass Transfer 42 (1999) 1979–1989.
[13] S. Wakashima, T.S. Saitoh, Benchmark solutions for natural convection in a cubic cavity using the high-order time-space methods, Int. J. Heat Mass Transfer 47 (2004) 853–864.
[14] N. Yucel, A.H. Ozdem, Natural convection in partially divided square enclosures, Heat Mass Transfer 40 (2003) 167–175.
[15] F. Ampofo, Turbulent natural convection in an air filled partitioned square cavity, Int. J. Heat Fluid Flow 25 (2004) 103–114.
[16] X. Shi, J.M. Khodadadi, Laminar natural convection heat transfer in a differentially heated square cavity due to a thin fin on the hot wall, J. Heat Transfer 125 (2003) 624–634.
[17] S. Ostrach, C. Raghavan, Effect of stabilizing thermal gradients on natural convection in rectangular enclosures, J. Heat Transfer 101 (1979) 238–243.
[18] G.S. Shiralkar, C.L. Tien, A numerical study of the effect of a vertical temperature difference imposed in a horizontal enclosure, Numer. Heat Transfer 5 (1982) 185–197.
[19] M.R. Ravi, R.A.W.M. Henkes, C.J. Hoogendoorn, On the high-Rayleigh-number structure of steady laminar natural-convection flow in a square enclosure, J. Fluid Mech. 262 (1994) 325–351.
[20] W. Wu, The effect of stable stratification on the natural convection in a square cavity caused by a horizontal temperature difference, Master's thesis, McMaster University, Hamilton, Ontario, Canada, 2004.
[21] R.B. Chinnakotla, D. Angirasa, R.L. Mahajan, Parametric study of buoyancy-induced flow and heat transfer from L-shaped corners with asymmetrically heated surfaces, Int. J. Heat Mass Transfer 39 (1996) 851–865.
[22] H.W. Coleman, W.G. Steele, Experimentation and Uncertainty Analysis for Engineers, second ed., Wiley, New York, 1999, pp. 48–50.
[23] Y.S. Tian, T.G. Karayiannis, Low turbulence natural convection in an air filled square cavity. Part I: The thermal and fluid flow fields, Int. J. Heat Mass Transfer 43 (2000) 849–866.
[24] R. Cheesewright, Natural convection from a plane, vertical structure in non-isothermal surroundings, Int. J. Heat Mass Transfer 10 (1967) 1847–1859.
[25] D.A.J. Olson, L.R. Glicksman, H.M. Ferm, Scale model studies of natural convection in enclosures with turbulent vertical boundary layers, in: R.S. Figliola, I. Catton (Eds.), Natural Convection in Enclosures, ASME HTD-vol. 63, 1986, pp. 17–24.